Proceedings of the 20th International Conference on Soil Mechanics and Geotechnical Engineering– Rahman and Jaksa (Eds)

Comparison of the AASHTO and EM methods for reinforced soil walls design under operational conditions

Comparaison des méthodes AASHTO et EM pour la conception de murs en sol renforcé en conditions opérationnelles

Seyed Hamed Mirmoradi & Mauricio Ehrlich
Department of civil engineering, COPPE, Federal University of Rio de Janeiro, Brazil, shm@ufrj.br

ABSTRACT: A main objective in the design of reinforced soil walls (RSWs) is the prediction of the maximum reinforcement load, T_{max}. Most currently used approaches for the design of RSWs are limit equilibrium (LE) methods or are based on the Rankine method [e.g., AASHTO 2017; Federal Highway Administration (FHWA) 2008] which have some important drawbacks. For example, these methods disregard the effects of reinforcement deformability, soil deformability, compaction, and in some cases cohesion. Working stress design methods have been developed to overcome these deficiencies and address more realistic approaches to the complex behaviour of reinforced soil structures (e.g., Ehrlich & Mitchell 1994; Ehrlich & Mirmoradi 2016). This paper investigates the prediction accuracy of the AASHTO simplified (2017) and the Ehrlich & Mirmoradi (2016) design methods considering different controlling factors such as wall height, facing, foundation and reinforcement stiffness, compaction-induced stress and toe restraint. Some limitations of each method are presented and discussed.

RÉSUMÉ: Un objectif principal de la conception de murs en sol renforcé (RSW) est la prédiction de la charge maximale de renforcement, Tmax. Les approches les plus couramment utilisées pour la conception des RSW sont des méthodes d'équilibre limite (LE) ou sont basées sur la méthode Rankine [par exemple, AASHTO 2017; Federal Highway Administration (FHWA) 2008] qui présentent d'importants inconvénients. Par exemple, ces méthodes ne tiennent pas compte des effets de la déformabilité des armatures, de la déformabilité du sol, du compactage et, dans certains cas, de la cohésion. Des méthodes de conception des contraintes de travail ont été développées pour surmonter ces lacunes et aborder des approches plus réalistes du comportement complexe des structures de sol renforcées (par exemple, Ehrlich et Mitchell 1994; Ehrlich et Mirmoradi 2016). Cet article étudie la précision de prédiction des méthodes de conception AASHTO simplifiées (2017) et Ehrlich & Mirmoradi (2016) en tenant compte de différents facteurs de contrôle tels que la hauteur du mur, le parement, la rigidité des fondations et des armatures, la contrainte induite par le compactage et la contrainte de pied. Certaines limites de chaque méthode sont présentées et discutées.

KEYWORDS: Reinforced soil walls, design methods, AASHTO simplified, EM (2016)

1 INTRODUCTION

Reinforced soil walls (RSWs) are widely utilized throughout the world as they have several advantages over other wall types, such as low cost, simple construction, and the ability to accommodate deformation. Prediction of the maximum reinforcement load, T_{max}, is a major objective in the design of reinforced soil structures. Most current methods, e.g., AASHTO (2017), used in RSWs design are limit equilibrium methods. In these methods, T_{max} is calculated by considering the forces required for local equilibrium, i.e., the tension strength of the reinforcements and the shear strength of the soil (e.g., Leshchinsky & Boedeker 1989).

Although these models are very simple to understand and use, they have some important drawbacks. In these methods, the effects of other controlling factors, such as reinforcement deformability, soil deformability, compaction, and in some cases cohesion, are simply disregarded (Mirmoradi & Ehrlich 2015b). Working stress design methods have been developed to address more realistic approaches to the complex behavior of reinforced soil structures (e.g, Ehrlich & Mirmoradi 2016, Ehrlich et al. 2017). The methods are based not only on analytical and case studies but also on studies of physical models in the laboratory.

The AASHTO (2017) simplified method is a limit equilibrium procedure that takes into consideration the influence of facing inclination and reinforcement stiffness for geosynthetics and steel. This method, however, does not consider the effects of the facing and apparent cohesion on the calculation. For calculations using this method, use of a direct shear and triaxial soil friction angle is recommended.

Ehrlich & Mirmoradi (2016) proposed an analytical procedure for the calculation of T_{max} under working stress conditions. This method explicitly takes into account the effect of compaction-induced stress, reinforcement and soil stiffness properties and facing inclination. The proposed method was based on Ehrlich & Mitchell's (1994) procedure. There are three key differences between the proposed method and Ehrlich & Mitchell's (1994) procedure: (1) the effect of the facing inclination is considered in the new method, while the original method was developed for vertical walls; (2) the calculation of T_{max} using the EM (2016) method does not need iteration, which was required by the original method; and (3) the equations are simpler to use. Depending on the wall's geometric condition, calculation using the EM (2016) design method can be performed using the plane strain or triaxial compression friction angles.

In this study, based on the results of the physical and numerical model studies, the prediction capabilities of the AASHTO simplified (2017) and EM (2016) design methods are investigated. This is carried out considering different controlling factors such as wall height, facing type and stiffness, foundation and reinforcement stiffness, compaction-induced stress and toe restraint.

2 EXPERIMENTAL STUDY

Instrument data and measurements from three physical model walls constructed at the Geotechnical Laboratory of COPPE/UFRJ are used. These walls are herein identified as Wall 1, Wall 2 and Wall 3. Figure 1 shows a cross-section and front view of Wall 1. The walls were constructed in a U-shaped concrete model box that is 1.5-m-high, 3.0-m-long, and 2.0-m-wide. The vertical spacing of reinforcements and the facing inclination were 0.4 m and 6° to the vertical, respectively.

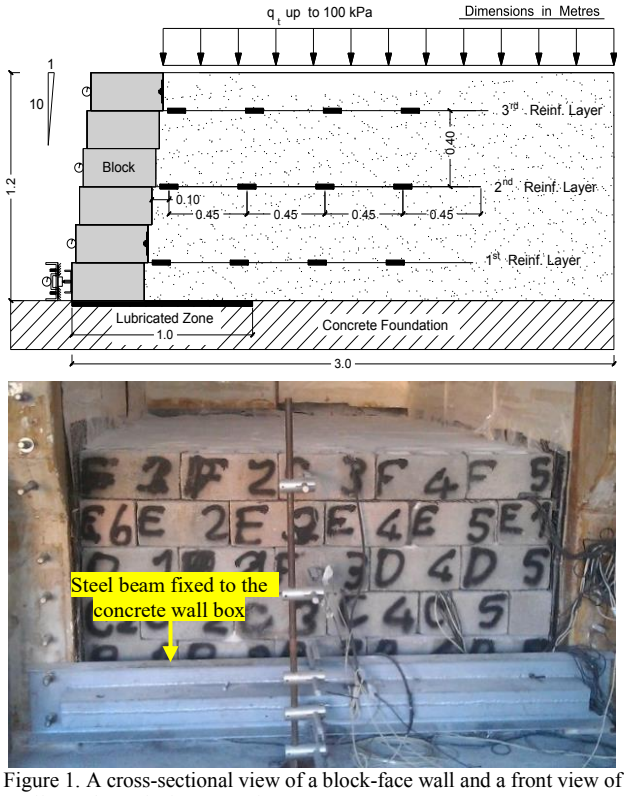

Figure 1. A cross-sectional view of a block-face wall and a front view of Wall 1 at the end of construction.

The height of the wall was 1.2 m. Three layers of geogrid were installed at 0.2 m, 0.6 m, and 1.0 m above the wall bottom. The reinforcements had a length of 2.12 m measured from the front of the wall face. Precast concrete blocks were used for the faces of the walls. The soil friction angles, determined by triaxial and plane strain tests on samples compacted to this unit weight, were 42º and 50º, respectively.

A 1-m-wide zone at the bottom of the walls, including the base of the block facing, was lubricated through a sandwich of rubber sheets and silicon grease, in order to allow for movement of the potential failure surface, keeping it away from the wall face. After construction, a surcharge loading of up to 100 kPa was applied over the entire surface of the backfill soil using an air bag.

The difference between Walls 1 and 2 were related to the toe conditions. In Wall 1, lateral movement of the toe was restricted by a steel beam fixed to the concrete U-shaped wall box, as shown in Figure 1. After the construction and application of the surcharge, the load was kept constant at 100 kPa. With the surcharge in place, the toe of Wall 1 was released step-by-step (0.5 mm horizontal movement allowed in each step).

The difference between Walls 2 and 3 were related to the compaction conditions. In walls 2 and 3 the backfill was compacted using a light vibrating plate (8 kPa) and vibratory tamper (63 kPa), respectively. Details of these three walls can be found in Ehrlich & Mirmoradi (2013), Mirmoradi & Ehrlich (2019) and Mirmoradi et al. (2016).

The reinforcement loads were measured using load cells installed at four points along each reinforcement layer. As shown in Figure 1 (two load cells at each point). The load cells were attached to the geogrid and measured the mobilised tension along the reinforcements. They allowed tension monitoring without the need to determine the reinforcement stress-strain curves, which are time dependent. The load cells were also capable of counterbalancing the temperature effects and the bending moments, and were strong enough to resist the stress induced during the operation of the compaction equipment (Ehrlich et al., 2012; Mirmoradi & Ehrlich 2018b, Mirmoradi et al., 2019).

2.1 *Test results*

Figure 2 compares the measured and calculated values of the summation of the maximum reinforcement loads ΣT_{max}, using the AASHTO simplified and EM (2016) design methods. Regarding the AASHTO simplified method, the calculations were performed employing the triaxial and plane strain soil friction angles. The results are shown during the surcharge application and toe release.

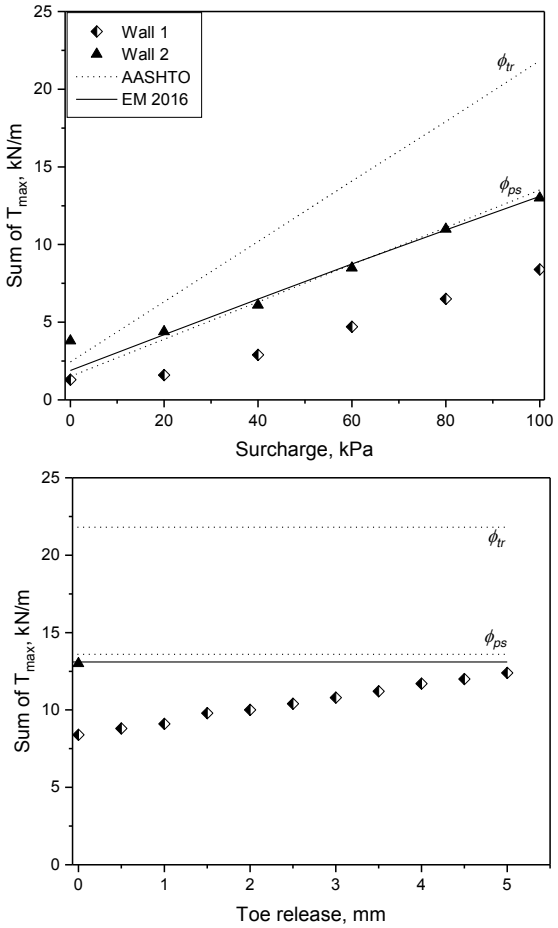

Figure 2. Comparison of the measured and calculated values of ΣT_{max} versus surcharge and toe release.

Figure 2 shows that, for Wall 1, the AASHTO simplified and the EM methods overestimate the reinforcement loads during the surcharge application. Considering the triaxial friction angle in the calculation, significant overestimation of the AASHTO method is observed compared to the measured values in Walls 1 (by over a factor of three). However, this overestimation decreases during toe release. Of note for Wall 1, is that the combined effect of facing stiffness and toe restraint leads to lower reinforcement loads. This effect is not considered in the AASHTO and EM (2016) methods. The figure indicates that, during the toe release, the influence of the block facing on the reinforcement load would vanish, and the accuracy of the AASHTO simplified and EM (2016) methods would increase.

In Wall 2, as no toe restraint was applied, facing effects do not occur. Therefore, as shown in Figure 2, the reinforcement load values measured in Wall 2 closely match those obtained by the AASHTO method using plane-strain friction angle and EM (2016) method.

Figure 3 compares the individual values of the maximum reinforcement loads T_{max}, measured for Walls 1 and 2 at the end of construction (EOC), under 100 kPa surcharge loading (EOL), and at the end of the toe release (EOR) with values calculated

using the AASHTO, and EM (2016) methods. Of note, the results presented for the AASHTO simplified method is consideing plane-strain friction angle the calculations. Results show that at EOC and EOL, the distribution of T_{max} with depth is more uniform for Wall 1. After toe release, however, the shape of the distribution of T_{max} with depth becomes triangular. For Wall 2, where there was no toe restraint from the beginning of the test, a similar triangular shape is observed.

Furthermore, this figure illustrates that the AASHTO and EM (2016) methods, in general, properly predict the values of T_{max} at EOC. At EOL, those methods overestimate the values of T_{max} for Wall 1. This discrepancy, however, decreases during toe release.

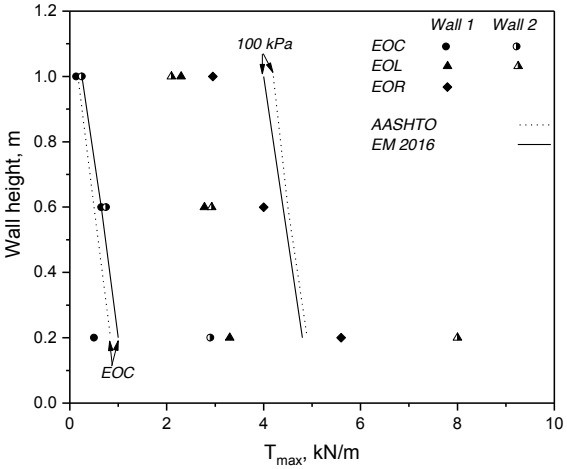

Figure 3. Comparison of measured and calculated values of Tmax versus depth for two walls.

Figure 4 compares the measured values of the summation of the maximum tension mobilized in the reinforcement, $\sum T_{max}$, with those determined by PLAXIS, the EM (2016) method, and the AASHTO simplified method. The equivalent depth of the soil layer (Z_{eq}) is defined by:

$$Z_{eq} = Z + q/\gamma \quad (1)$$

where Z and q are the real depth of a specific layer and the surcharge load value of the physical model, respectively. As shown in Figure 4, the values measured from the physical model were properly captured by the EM (2016) method, and the numerical analysis. Additionally, when plane-strain friction angle was used, the AASHTO simplified method underpredicts the measured values, which is more pronounced for the lower values of Z_{eq}. Additionally, using triaxial friction angle, the AASHTO simplified method, overestimates $\sum T_{max}$ for $Z_{eq}>2$.

3 NUMERICAL STUDY

Numerical modelling was performed for block-face and wrapped-face MSE walls using the 2D finite element program PLAXIS (Brinkgreve & Vermeer, 2002). Details about the validation of the models can be found in Mirmoradi & Ehrlich (2014a, b, 2015a, 2018a), Mirmoradi et al. (2020) and Nascimento et al. (2020).

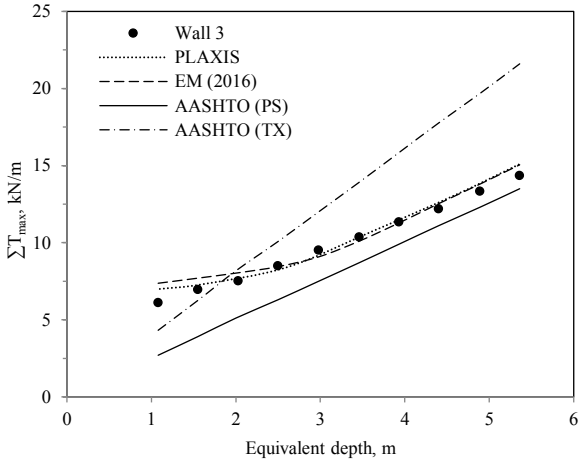

Figure 4. Comparison of measured and determined summations of the maximum reinforcement loads.

Parametric studies were carried out to evaluate the combined effects of facing stiffness, reinforcement stiffness, toe fixity, and wall height. Three different wall heights were considered: 4, 8, and 16 m. The length and the vertical spacing of reinforcements were 0.7 H and 0.4 m, respectively. Block facing with vertical facing inclination was considered. Two different toe fixity conditions were considered (free and fixed base conditions), and a hardening soil model was applied.

The backfill compaction was modeled by applying an 8-kPa distribution load at the top and bottom of each soil layer (Mirmoradi & Ehrlich 2015a, b, Scotland et al. 2016, Linhares et al. 2021). A fixed boundary condition in the horizontal direction was employed on the right lateral border. At the bottom of the model, a fixed boundary condition in both the horizontal and vertical directions was applied. For the models with free-base conditions, a fixed boundary condition in the vertical direction was employed at the bottom of the block facing.

Reinforcement was modelled as a linear elastic material with perfect interface adherence to the adjacent soil. Several studies showed that under working stress conditions, the assumption of perfect adherence results in an agreement between calculated values and measured results (e.g., Dyer & Milligan 1984, Jewell 1980, Ehrlich & Mitchell 1994, Holtz & Lee 2002, Hatami & Bathurst 2005, Guler et al. 2007, Ehrlich et al. 2021).

Three values of the tensile stiffness modulus of reinforcement J_r, equal to 600, 6000, and 60000 kN/m, were employed. Assuming these values, the relative soil-reinforcement stiffness index S_i, equal to 0.025, 0.25, and 2.5, was calculated. The parameter Si was developed by Ehrlich & Mitchell (1994) and can be calculated as follows:

$$S_i = J_r/kS_vP_a \quad (2)$$

where k is the modulus number (hyperbolic stress-strain curve model), P_a is the atmospheric pressure, and S_v is the vertical reinforcement spacing. Table 1 provides the input parameters used in the numerical analyses. The reader is directed to the paper by Mirmoradi & Ehrlich (2015b, 2017) for additional information about numerical modeling.

3.1 *Numerical study results*

Figure 5 compares the normalized values of the summation of the maximum tension in the reinforcements and the normalized facing stiffness using the values calculated by the PLAXIS computer model, the EM (2016) method and the simplified method of AASHTO (2017). Figure 5 shows the results for different toe conditions (i.e., fixed-base and free-base), and the

following three different wall heights: 4, 8, and 16 m. Additionally, the relative soil-reinforcement stiffness index S_i is equal to 0.025.

Table 1. Input parameters for the parametric study.

Property	Value
Soil property	
Model	Hardening Soil
Peak plane strain friction angle, ϕ, (o)	50
Cohesion, c, (kPa)	1.0
Unit weight, γ, (kN/m3)	20
Eref50, (kPa)	42500
Erefoed, (kPa)	31800
Erefur, (kPa)	127500
Stress dependence exponent, m	0.5
Failure ratio, Rf	0.9
Poisson's ratio, υ	0.2
Modular block properties	
Model	Linear elastic
Size, (m×m)	0.4×0.2
Unit weight, γ, (kN/m3)	22
Stiffness modulus, (kPa)	1×10^6
Poisson's ratio, υ	0.15
Block-block interface	
Friction angle, ϕ, (o)	57
Cohesion, (kPa)	46
Soil-block interface	
Friction angle, ϕ, (o)	44
Cohesion, (kPa)	1
Dilation angle, Ψ, (o)	11

For the free-base condition, the results determined using PLAXIS were quite similar to the values predicted using the method of EM (2016) and the AASHTO simplified method, in which the plane-strain friction angle was utilized. Additionally, when triaxial friction angle was employed in the AASHTO calculation, this method significantely overpredicted the determined values by PLAXIS. As shown in Figure 5, both methods overpredict the values calcultaed for the models with fixed-base conditions. Nevertheless, the descripancy between the calculated values by PLAXIS for the fixed-base conditions and the design methods decrease with wall height.

Fixed-base and free-base conditions are the upper and lower bounds of the possible conditions found in the field. It is important to notice that in this study, the effect of the toe restraint was fundamentally evaluated considering a wide range of lateral displacements at the toe of the block face. In real field conditions, the toe of the block facing with no lateral restriction may not occur. It may not also be possible to restrict the lateral displacement fully at the toe of the block face walls. It means that the behavior of actual field conditions is between those two upper and lower bonds. Depending on the foundation of the block-facing, this behavior could be closer to the fix or free toe conditions (Mirmoradi & Ehrlich 2016).

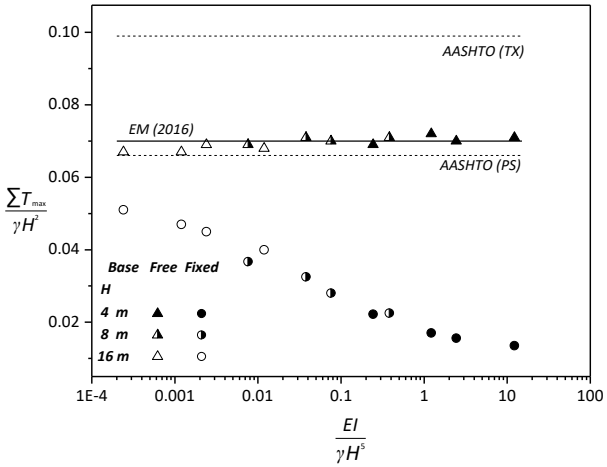

Figure 5. Comparison of measured and calculated values of T_{max} versus depth for two walls.

Moreover, as shown by Mirmoradi & Ehrlich (2015b), the combined effect of the facing stiffness and toe restraint substantially depends on the height of the reinforced soil walls. When the height of the wall increases, the effect of the facing stiffness and toe restraint on the reinforcement load would significantly decrease. Therefore, the practice of ignoring the toe restraint produced by a 0.3–0.5 m-deep block may be justified in the design, to increase the margin of safety against reinforcement overstressing in the case here lateral movements of the toe blocks occur.

Figure 6 presents the normalised values of T_{max} versus wall height for the models with 4 m and 8 m heights, for wrapped and block facings and with different foundation stiffness. The figure shows that for the wrapped-face wall, the variation in the foundation stiffness did not affect T_{max} for either wall height, whereas for the block-faced walls, the influence of foundation stiffness on T_{max} and its importance decreased with wall height, as discussed above.

Figure 6 also shows that for walls with different facing types, the influence of the facing on the magnitude of T_{max} decreased with wall height. For the 4 m high wall, when the block face was modelled, T_{max} was influenced by the stiffness of the block facing with values lower than the corresponding K_a line, except for the top reinforcement layer. When the wrapped face was employed, the maximum loads in the reinforcement layers were well represented by the K_a line up to a certain depth; followed by a decrease in the layers located near the foundation due to the influence of foundation restriction on reinforcement load mobilisation. For the 8 m high wall, T_{max} at the upper half of the walls was practically the same and was well represented by the K_a line (almost 3 m above the base of the wall) for both block- and wrapped-face walls. Below 3 m, a greater reduction in T_{max} in the reinforcements was observed for the block facing rather than the wrapped facing due to the combined effects of facing stiffness and toe restriction. These findings are supported by the relative facing stiffness index, $EI/\gamma H^5$, as presented by Mirmoradi & Ehrlich (2015b), which decreases for tall walls.

Figure 6 compares the results of the numerical analyses and the values calculated using the design methods. The figure shows that the AASHTO simplified method overestimates T_{max} determined by PLAXIS, which is more pronounced for the shorter wall (i.e., 4 m wall). This was also observed in the results

presented by Yu et al. (2017), who compared the measured values of T_{max} for 3.6 m high wrapped-face physical models with the calculated values from numerical analyses and the AASHTO simplified method. The overestimated values calculated using this method were principally due to the value of the soil friction angle used in the calculation. This can be seen when comparing the results of the numerical analyses with the corresponding K_a line, which also represent the AASHTO simplified method considering the plane-strain friction angle. Moreover, Figure 6 illustrates that the EM (2016) method well represents the T_{max} values of the wrapped-face wall in all reinforcement layers with the exception of layers placed close to the wall bottom. Note that this method does not consider the effect of facing stiffness and toe restraint in its calculation.

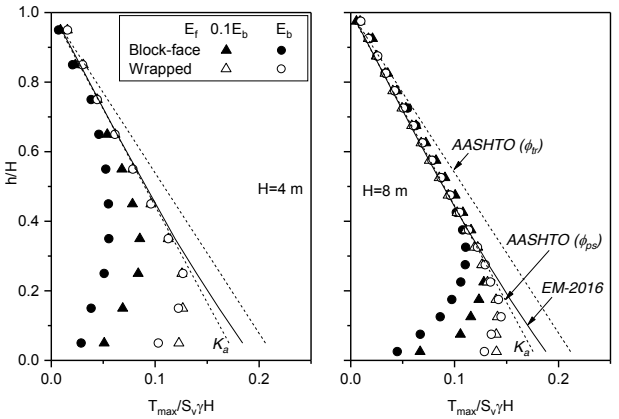

Figure 6. Comparison of measured and calculated values of T_{max} versus depth for two walls.

Figures 7 and 8 compare the values of the distribution of the maximum reinforcement load for different wall heights and reinforcement stiffness values calculated by PLAXIS for the fixed-base conditions, the Ehrlich & Mirmoradi (2016) and AASHTO simplified methods. Figure 7 shows that for a given wall height, decreasing the reinforcement stiffness leads to more uniform distribution of the reinforcement load with depth. This is consistent with the results presented by Ho & Rowe (1992). This also implies that increasing S_i results in changes the shape of the distribution of the reinforcement load from trapezoidal to triangular. Note that the triangular shape of distribution is more pronounced for taller walls, as previously discussed. Furthermore, there is not a significant difference between the reinforcement load for different Si values near the wall top, as shown in previous studies (e.g., Rowe & Ho, 1997; Ehrlich & Mitchell, 1994).

Fig. 7 compares the results calculated using PLAXIS and the EM (2016) method. This figure shows that the predictability of the EM method increases for models with a lower facing effect that occurs for a greater wall height and S_i. This figure shows that the EM (2016) method may overpredict the reinforcement load in layers ~4 m above the base of the wall for a wall with fixed-base conditions. This is regardless of the wall height. As disscussed by Mirmoradi and Ehrlich (2017) and Mirmoradi et al. (2021), for vertical RSWs with segmental block facing, the combined effect of the facing and reinforcement stiffness, wall height, and toe resistance on the distribution of the maximum reinforcement load with depth may be limited to approximately 4 m above the base of the wall. This is in agreement with the results presented by Ho and Rowe (1992), Liu and Won (2009), and Jiang et al. (2019).

Figure 8 shows that, using the triaxial soil friction angle, the AASHTO simplified method overestimates the reinforcement loads for the walls in which the polymeric reinforcements were used, especially for the conventional geosynthetic reinforcement (Si = 0.025). For the steel reinforcement (i.e., Si = 2.5), this method better represents Tmax determined by PLAXIS. Additionally, for the high wall, this method shows a better representation of T_{max}, due to the reduction of the facing influence on the reinforcement loads.

Figure 8 also shows that when plane-strain soil friction angle is used in the calculation, the AASHTO simplified method represents T_{max} determined by PLAXIS for the conventional geosynthetic (S_i = 0.025) well, except for the reinforcement layers where block facing affects the reinforcement loads. For S_i of 0.25 and 2.5, Figure 8 shows the underprediction of the AASHTO simplified method for taller walls (8 m and 16 m).

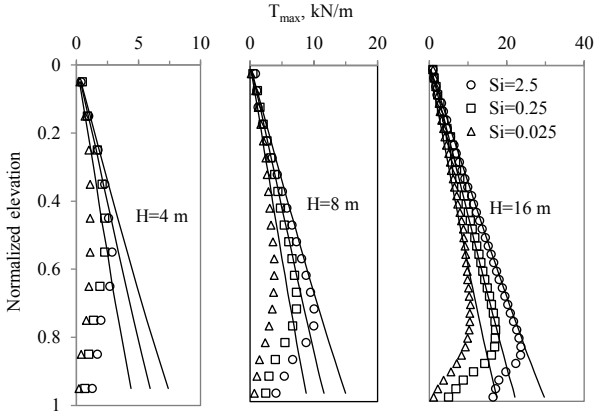

Figure 7. Reinforcement load versus normalized elevation for different wall height and reinforcement stiffness. Solid lines: Ehrlich and Mirmoradi method.

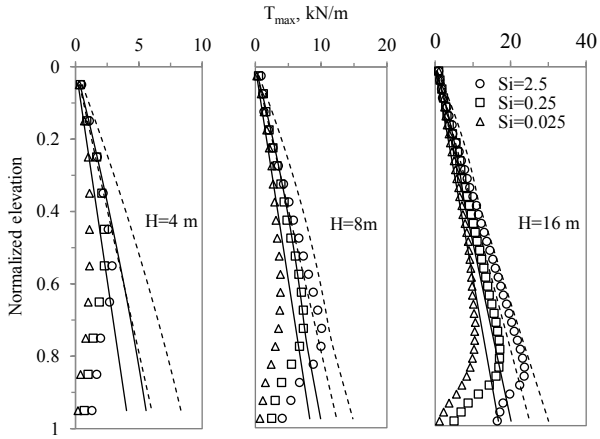

Figure 8. Reinforcement load versus normalized elevation for different wall height and reinforcement stiffness. Solid lines and dashed lines represent the AASHTO method using plane strain and triaxial friction angles, respectively.

4 CONCLUSIONS

The prediction capabilities of the AASHTO (2017) simplified and EM (2016) design methods have been investigated using data from physical and numerical model studies. The results indicate that these capabilities may be significantly influenced by the combined effect of the facing, reinforcement and foundation stiffness, toe resistance, wall height, and compaction-induced stress.

In this study, the key factors that strongly affect Tmax prediction accuracy of the AASHTO simplified method are:

I) disregard for the combined effect of facing stiffness and toe restraint,
II) disregard for the effect of CIS,
III) use of the peak triaxial or direct shear friction angle in the calculations for all cases including those in which the plane-strain conditions govern, and

IV) the lateral earth pressure coefficient employed for the stiff polymeric and steel-reinforced wall.

The T_{max} prediction accuracy of the EM (2016) method, which is a simplified version of the method proposed by Ehrlich & Mitchell (1994), principally depends on wall height, facing stiffness, toe resistance and foundation conditions. For a given reinforcement stiffness, this method, in general, predicts T_{max} in all layers in which the load in the reinforcement is not affected by the combined effect of facing stiffness and toe restraint. Therefore, increasing the wall height and/or reducing toe restraint increases the accuracy of this method because the effect of facing stiffness and toe restraint is not considered. Additionally, depending on the wall's geometric condition, calculations using the EM (2016) design method can be performed using the plane-strain or triaxial friction angles. In this method, the facing inclination and compaction-induced stress are also explicitly considered in the calculations.

5 ACKNOWLEDGEMENTS

The authors greatly appreciate the funding for this study provided by the Brazilian Research Council, CNPq, and the Brazilian Federal Agency for Support and Evaluation of Graduate Education, CAPES. We also thank Flavio Montez and Andre Estevao Ferreira da Silva from the Huesker Company for their support.

6 REFERENCES

AASHTO, 2017. AASHTO LRFD bridge design specifications. *American Association of State Highway and Transportation* Officials, 8th edn. Washington, D.C., USA.

Brinkgreve, R. B. J., and Vermeer, P. A. (2002). PLAXIS: *Finite element code for soil and rock analyses*, version 8, CRC Press/Balkema, Leiden, Netherlands.

Dyer N. R. and Milligan G. W. E. (1984). A photoelastic investigation of the interaction of a cohesionless soil with reinforcement placed at different orientations. *Proc., Int. Conf. on In-Situ Soil and Rock Reinforcement*, International Society of Soil Mechanics and Geotechnical Engineering (ISSMGE), London, 257–262.

Ehrlich M. and Mirmoradi S. H. 2013. Evaluation of the effects of facing stiffness and toe resistance on the behavior of GRS walls, *J. Geotextile Geomembr.*, 40(Oct), 28–36.

Ehrlich M. and Mirmoradi S. H. 2016. A simplified working stress design method for reinforced soil walls, *Géotechnique*, 66(10), 854–863.

Ehrlich M., Mirmoradi S.H. and Xu D. S., 2017. A simplified working stress design method for reinforced soil walls. *Geotechnique*, 67 (11), 1029-1032.

Ehrlich M., Mirmoradi, S.H. and Saramago R.P. 2012. Evaluation of the effect of compaction on the behavior of geosynthetic-reinforced soil walls. J. *Geotextile Geomembr*. 34, 108–115.

Ehrlich, M., Mirmoradi, S.H., Tortureli, M., 2021. Numerical evaluation of backfill compaction behind the face of reinforced soil walls. Proceedings of the Institution of Civil Engineers - Geotechnical Engineering 1–12. https://doi.org/10.1680/jgeen.20.00246.

Ehrlich M. and Mitchell J.K., 1994. Working stress design method for reinforced soil walls. *J. Geot. Eng. ASCE* 120 (4), 625–645.

Federal Highway Administration (FHWA). 2008. Geosynthetic design and construction guidelines. *FHWA NHI-07-092*, Washington, DC.

Guler E., Hamderi M. and Demirkan M.M., 2007. Numerical analysis of reinforced soil retaining wall structures with cohesive and granular backfills. *Geosynth. Int.* 14 (6), 330–345.

Hatami K. and Bathurst R.J. 2005. Development and verification of a numerical model for the analysis of geosynthetic-reinforced soil segmental walls under working stress conditions, *Canadian eotechnical Journal*, 42(4), 1066–1085.

Holtz R.D. and Lee W. F. 2002. WA-RD 532.1: Internal Stability Analyses of Geosynthetic Reinforced Retaining Walls., *Washington State Transportation Center* (TRAC). Seattle, Washington. USA.

Ho S.K. and Rowe, R.K., 1992. Finite element analysis of geosynthetic reinforced soil walls. *In: Geosynthetic 93 Conference*, Vancouver.

Jewell R.A. 1980. Some effects of reinforcement on the mechanical behavior of soils. *Ph.D. thesis*, Univ. of Cambridge, Cambridge, U.K.

Jiang Y., Han J., Zornberg J., Parsons R. L., Leshchinsky D. and Tanyu B., 2019. Numerical Analysis of Field Geosynthetic-Reinforced Retaining Walls with Secondary Reinforcement. *Geotechnique*, 69(2), 122-132.

Leshchinsky D. and Boedeker R. H. 1989. Geosynthetic reinforced structures. *J. Geotech. Engrg*., 115: 10(1459), 1459–1478.

Linhares, R.M, Mirmoradi, S.H., Ehrlich, M., 2021. Evaluation of the effect of surcharge on the behavior of geosynthetic-reinforced soil walls. Transportation Geotechnics 100634. https://doi.org/10.1016/j.trgeo.2021.100634.

Liu H. and Won M.S., 2009. Long-term reinforcement load of geosynthetic-reinforced soil retaining walls. *J. Geotech. Geoenviron. Eng*. ASCE 135 (7), 875-889.

Mirmoradi S.H. and Ehrlich M., 2014a. Modeling of the compaction-induced stresses in numerical analyses of GRS walls. *Int. J. Comput. Methods (IJCM)* Special Issue "Comput. Geomech." 11 (2), 14.

Mirmoradi S.H. and Ehrlich M., 2014b. Geosynthetic reinforced soil walls: experimental and numerical evaluation of the combined effects of facing stiffness and toe resistance on performance. *In: Proc., 10th Int. Conf. on Geosynthetics,* International Society of Soil Mechanics and Geotechnical Engineering (ISSMGE), London.

Mirmoradi S.H. and Ehrlich M. 2015a. Modeling of the Compaction-induced Stress on Reinforced Soil Walls. *J. Geotextile Geomembr*. 43 (1), 82-88.

Mirmoradi S.H. and Ehrlich M. 2015b. Numerical evaluation of the behavior of GRS walls with segmental block facing under working stress conditions. *J. Geotech. Geoenviron. Eng.* ASCE 141 (3), 04014109.

Mirmoradi S.H. and Ehrlich, M. 2016. Evaluation of the effect of toe restraint on GRS walls. *Transp. Geotech*. SI Geosynthetics in Tpt. 8, 35-44.

Mirmoradi S.H. and Ehrlich, M. 2017. Effects of facing, reinforcement stiffness, toe resistance, and height on reinforced walls. *J. Geotextile Geomembr.* 45 (1): 67–76.

Mirmoradi S.H. and Ehrlich M. 2018a. Numerical simulation of compaction-induced stress for the analysis of RS walls under working conditions, *J. Geotextile Geomembr*., 46(3), 354–365.

Mirmoradi S.H. and Ehrlich M. 2018b. Experimental evaluation of the effect of compaction near facing on the behavior of GRS walls, *J. Geotextile Geomembr*., 46(5), 566-574.

Mirmoradi S.H., Ehrlich M. and Dieguez, C. 2016. Evaluation of the combined effect of toe resistance and facing inclination on the behavior of GRS walls, *J. Geotextile Geomembr.*, 44, 287–294.

Mirmoradi S.H. and Ehrlich M. 2019. Experimental Evaluation of the Effects of Surcharge Width and Location on GRS Walls, *International Journal of Physical Modelling in Geotechnics*, 19(1): 27-36.

Mirmoradi S.H., Ehrlich M., Chinchay P. and Dieguez C. 2019. Evaluation of the combined effect of facing inclination and uniform surcharge on GRS walls, *J. Geotextile Geomembr*, 103485.

Mirmoradi, S.H., Ehrlich, M., Nascimento, G., 2020. Experimental, numerical, and analytical investigation of the effect of compaction-induced stress on the behavior of reinforced soil walls. Soils and Rocks 43, 419–439.

Mirmoradi, S.H., Ehrlich, M., Magalhães, L.F.O., 2021. Numerical evaluation of the effect of foundation on the behavior of reinforced soil walls. Geotextiles and Geomembranes 49, 619–628.

Nascimento G., Ehrlich M. and Mirmoradi S.H., 2020. Numerical-simulation of compaction-induced stress for the analysis of RS walls under surcharge loading, *J. Geotextile Geomembr*., 48(4), 532-538.

Rowe, R.K., Ho, S.K., 1997. Continuous panel reinforced soil walls on rigid foundations. J. Geotech. Geoenviron. Eng. 123 (10), 912–920.

Scotland I., Dixon N., Frost M., Fowmes G. and Horgan, G. 2016. Modelling deformation during the construction of wrapped geogrid-reinforced structures. *Geosynth. Int*. 23 (3), 219–232.

Yu Y., Bathurst R.J. and Allen T.M. 2017. Numerical Modelling of two full-scale reinforced soil wrapped-face walls. *J. Geotextile Geomembr*., 45(4): 237-249.